# Change of Electronic Structure in $Ca_2RuO_4$ Induced by Orbital Ordering

J. H. Jung,[1] Z. Fang,[1,2] J. P. He,[1] Y. Kaneko,[1] Y. Okimoto,[3] and Y. Tokura[1,3,4]

[1]*Spin Superstructure Project, ERATO, Japan Science and Technology Corporation (JST), Tsukuba 305-8562, Japan*

[2]*Institute of Physics, Chinese Academy of Science, Beijing 100080, China*

[3]*Correlated Electron Research Center (CERC), National Institute of Advanced Industrial Science and Technology (AIST), Tsukuba 305-0046, Japan*

[4]*Department of Applied Physics, University of Tokyo, Tokyo 113-8656, Japan*

(Received 26 September 2002; published 31 July 2003)

Optical conductivity spectra $\sigma(\omega)$ were used to investigate the effect of orbital ordering on the electronic structure of $Ca_2RuO_4$. Our LDA + $U$ calculation predicts Ru $4d_{xy}$ *ferro-orbital* ordering at the ground state, and well explains the present $\sigma(\omega)$ as well as the reported O $1s$ x-ray absorption spectra. Variation of temperature ($T$) causes a large change of spectral weight over several eV as well as collapse of a charge gap accompanied by elongation of the $c$-axis Ru-O bond length. These results clearly indicate that the $d_{xy}$ orbital ordering plays a crucial role in the metal-insulator transition and the $T$-dependent electronic structure on a large energy scale.

DOI: 10.1103/PhysRevLett.91.056403 PACS numbers: 71.30.+h, 75.50.Ee, 78.30.–j

During the past several years, considerable interest has been focused on the origin and nature of a complex phase diagram shown in single-layered ruthenates $Ca_{2-x}Sr_xRuO_4$ [1]. The end members $Sr_2RuO_4$ and $Ca_2RuO_4$ have been known to be a spin-triplet superconductor [2] and an antiferromagnetic insulator [3,4], respectively. It has been shown that the evolution of physical properties with $x$ is nonmonotonous, and a close relationship among electrical, magnetic, and structural properties does exist [5,6]. In addition, recent experimental and theoretical works have suggested an important role of the orbital degree of freedom [7–11].

Despite extensive studies, controversy persists regarding the understanding of the electronic structure of $Ca_2RuO_4$ in the ground state, especially with respect to the role of the orbital degree of freedom. It is naturally expected that the $d_{xy}$ orbital should be dominantly occupied (hereafter, we call this the $d_{xy}$ orbital ordering) due to the tetragonal crystal field effect. However, Mizokawa *et al.* [9] estimated 0.5 holes in the $d_{xy}$ orbital and 1.5 holes in the $d_{yz/zx}$ orbital using angle dependent O $1s$ x-ray absorption spectra. With the estimated hole distributions, they argued that the ground state may favor the occupation of complex orbitals due to the strong spin-orbit coupling. In addition, Hotta and Dagotto [10] proposed an antiferro-(staggered-)orbital ordering model that results in the doubling of the unit cell. Moreover, Lee *et al.* [11] suggested the coexistence of antiferro- and ferro-orbital ordering in their optical study. Thus, the clear understanding of electronic structure of $Ca_2RuO_4$ is still left to be established. In this Letter, we report the systematic investigations using optical spectroscopy and theoretical LDA + $U$ calculation for the orbital degree of freedom. Our results clearly indicate that the $d_{xy}$ *ferro-orbital* ordering occurs at the ground state in contrast to previous proposals, and causes the strong temperature ($T$) dependence of electronic structure including the hole population change and the metal-insulator transition of this compound.

Single crystals of $Ca_2RuO_4$ were grown by the floating-zone method. Polycrystalline rods were prepared with the 3:2 M ratios of $CaCO_3$ and $RuO_2$ at 1350 °C. Using a halogen lamp image furnace under 8 atm $O_2$ pressure, the crystal was successfully grown without any trace of impurity. $T$-dependent magnetic susceptibility and resistivity were measured with the use of a superconducting quantum interference device magnetometer with 1 T after zero field cooling and a four-probe method, respectively.

Near-normal-incidence reflectivity spectra $R(\omega)$ were measured for 0.06–36 eV on the $ab$ plane ($E\|ab$) and along the $c$ axis ($E\|c$) in a $T$ range between 10 to 400 K during a cooling run. Optical conductivity spectra $\sigma(\omega)$ were obtained by the Kramers-Kronig transformation of $R(\omega)$. For the transformation, room-$T$ $R(\omega)$ data for $5\ \text{eV} \leq \hbar\omega \leq 36\ \text{eV}$ were connected to $T$-dependent $R(\omega)$ data below 5 eV and $\omega^{-4}$ dependence was assumed above 36 eV. We also assumed a constant $R$ or Hagen-Rubens relation below 0.06 eV, and found that $\sigma(\omega)$ above 0.15 eV were nearly independent of extrapolations. The Raman spectra were taken with the use of a 632.8 nm line from a He-Ne laser. The backward scattered light was collected and dispersed by a monochromator equipped with a charge-coupled-device detector.

Figure 1(a) shows the $T$-dependent magnetic susceptibility ($\chi_{ab}$) and dc resistivity ($\rho_{ab}$) for the $ab$ plane. At low $T$ ($< T_N = 110$ K), $Ca_2RuO_4$ shows an antiferromagnetic spin ordering and an insulating electrical behavior. The $T$ variation of the Ru-O bond lengths [$d$(Ru-O)] obtained by a neutron scattering measurement as reported by Friedt *et al.* [5] is shown in Fig. 1(b). The $RuO_6$ octahedra are flattened at low $T$, i.e., $d[\text{Ru-O(1)}]/d[\text{Ru-O(2)}] > 1.02$, where $d$[Ru-O(1)] and $d$[Ru-O(2)] represent the in-plane and apical bond lengths, respectively. With increasing $T$, the

  

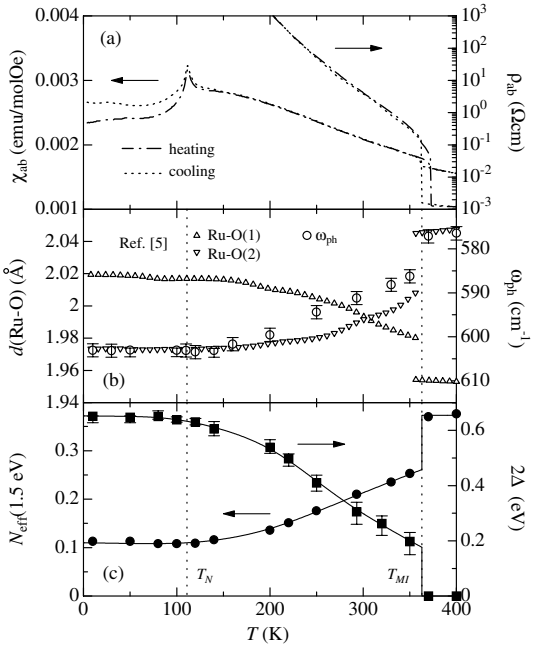


FIG. 1. Temperature-dependent (a) in-plane magnetic susceptibility $\chi_{ab}$ and resistivity $\rho_{ab}$, (b) in-plane Ru-O(1), apical Ru-O(2) bond lengths [Ref. [5]], and apical oxygen phonon frequency $\omega_{\rm ph}$, and (c) effective number of electrons $N_{\rm eff}$ (1.5 eV) and optical gap $2\Delta$ of $Ca_2RuO_4$. In (c), the solid lines are guides for the eyes.

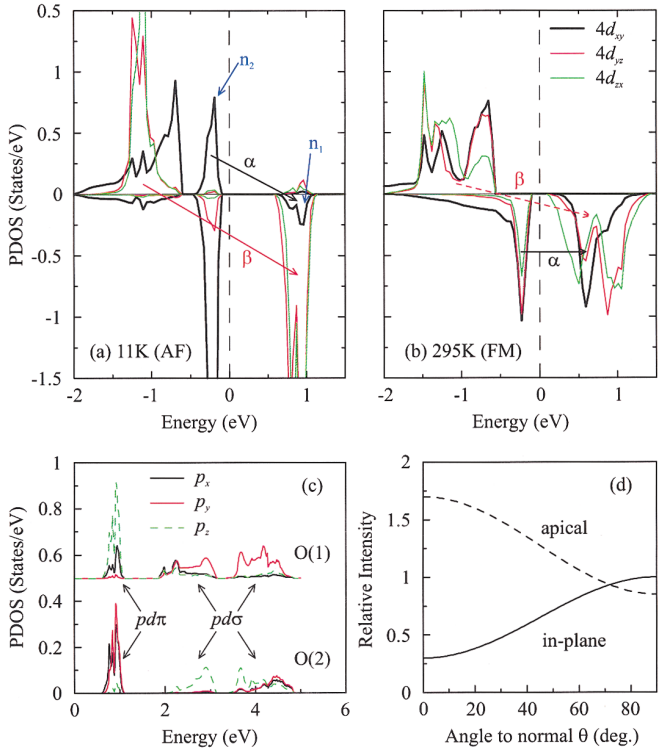


FIG. 2 (color). Projected density of state (PDOS) for Ru $t_{2g}$ calculated using (a) the 11 K crystal structure with antiferromagnetic (AF) spin state and (b) the 295 K crystal structure with ferromagnetic (FM) spin state, and PDOS for (c) in-plane oxygen O(1) and apical oxygen O(2) at 11 K (AF). (d) Relative intensity for in-plane and apical component of x-ray absorption peak with respect to incident angle $\theta$. In (a) and (b), $\alpha$ and $\beta$ represent the possible optical transitions. $n_1$ and $n_2$ in (a) represent the $d_{xy}$ states originating from rotation/tilting and hybridization.

paramagnetic insulating state appears with regularization of $RuO_6$ octahedra, i.e., the monotonous decrease and increase of $d$[Ru-O(1)] and $d$[Ru-O(2)], respectively. At high $T$ ($> T_{MI} \equiv 363$ K), sharp drops of $\chi_{ab}$ and $\rho_{ab}$ occur [12] accompanying sudden changes of $d$(Ru-O). The transition is of the first order as noticed in a large hysteresis of $\chi_{ab}$ and $\rho_{ab}$; it occurs at 372 K with heating and 363 K with cooling. Above $T_{MI}$, $\rho_{ab}$ is as low as $10^{-3}$ Ω cm and nearly $T$ independent, while $\chi_{ab}$ is slowly decreased. The state may be viewed as barely metallic similar to other layered ruthenates [13]. These systematic features show the strong correlation among charge, spin, and lattice degrees of freedom in $Ca_2RuO_4$.

To gain insights into the electronic structure, we performed the first-principles calculations based on the LDA + $U$ scheme with an effective Coulomb repulsion parameter ($U_{\rm eff} = 3.0$ eV) [14] and the experimental crystal structures [15]. Figure 2(a) shows the projected density of state (PDOS) to three Ru $t_{2g}$ orbitals calculated using the 11 K crystal structure with antiferromagnetic spin order [hereafter, denoted as 11 K (AF)]. Among four electrons in Ru 4$d$, three electrons occupy the $d_{xy}$ (black lines), $d_{yz}$ (red lines), and $d_{zx}$ (green lines) orbitals with majority spins. A remaining electron predominantly occupies the $d_{xy}$ orbital with minority spin, giving the $d_{xy}$ ferro-orbital ordering. (It is demonstrated that the inclusion of spin-orbit coupling does not affect the orbital occupation significantly, as discussed elsewhere [16].)

Important features in the PDOS are the strong mutual mixture of $t_{2g}$ orbitals due to the rotation/tilting of $RuO_6$ octahedra and also to the extended nature of Ru 4$d$ states. It results in a finite hole count of the $d_{xy}$ orbital (as indicated by $n_1$) in the $d_{yz/zx}$ orbital band and a substantial distribution of the majority spin $d_{xy}$ state (as indicated by $n_2$) at the energy of the minority spin $d_{xy}$ state. Figure 2(b) shows the PDOS to three Ru $t_{2g}$ orbitals calculated using the 295 K crystal structure with a ferromagnetic spin state [hereafter, denoted as 295 K (FM)]. As noticed, the hole population of $d_{xy}$ is strongly enhanced while that of $d_{yz/zx}$ is suppressed. It suggests the crucial change of electronic structure by elongation of the $RuO_6$ octahedra and the change of spin configuration.

Figure 2(c) shows the PDOS to O 2$p$ at 11 K (AF), which is hybridized with the unoccupied Ru $t_{2g}$ states ($pd\pi$ bonds) and Ru $e_g$ states ($pd\sigma$ bonds). Using this PDOS, we calculate the relative intensity of two peaks, observed in the O 1$s$ absorption experiment at 528.5 and 529.5 eV [9], as a function of light incident angle $\theta$ in Fig. 2(d). Since we are treating the transition from O 1$s$ to

O $2p$ states, the angle dependence of relative intensity of the peak for the in-plane and the apical part can be estimated as $\frac{1}{2}(\cos^2\theta + 1)(n_{p_x}^{(1)} + n_{p_y}^{(1)}) + \frac{1}{2}(\sin^2\theta)(2n_{p_z}^{(1)})$ and $\frac{1}{2}(\cos^2\theta + 1)(n_{p_x}^{(2)} + n_{p_y}^{(2)})$, respectively. Here $n_{p_x}$, $n_{p_y}$, and $n_{p_z}$ are the integrated unoccupied weight of three O $2p$ states, and the superscripts (1) and (2) indicate in-plane oxygen O(1) and apical oxygen O(2), respectively. The calculated result can qualitatively reproduce the experimental data at 90 K [9] without assuming 0.5 holes in the $d_{xy}$ orbital and 1.5 holes in the $d_{yz/zx}$ orbital, suggesting the validity of our calculation.

Using the Kubo formula, we calculated the optical conductivity spectra $\sigma(\omega)$ for $E\|ab$ [Fig. 3(a)] and $E\|c$ [Fig. 3(b)] at 11 K (AF) (solid lines) and 295 K (FM) (dashed lines). The calculated $\sigma(\omega)$ at 11 K (AF) show apparent three peaks for $E\|ab$ and one major peak for $E\|c$, and well reproduce the experimental $\sigma(\omega)$ at 10 K (see Fig. 4). Based on the calculated PDOS in Fig. 2(a), the origin of each peak in $\sigma(\omega)$ can be interpreted as follows. The strong and broad peaks near 3.5 eV for $E\|ab$ and $E\|c$ can be understood as the charge-transfer transition from O $2p$ to Ru $4d$. These transitions should mostly contribute to the spectral weight above 3 eV. The different peak positions for $E\|ab$ and $E\|c$ are due to the difference in the O $2p$ energy levels for in-plane and apical oxygen. In $E\|ab$, two more peaks are observed near 1.0 and 2.4 eV below the charge-transfer peak. They mostly come from the Ru $d$-$d$ transitions. The weak peak $\alpha$ and intense peak $\beta$ can be understood as the transition from the occupied $d_{xy}$ on one Ru site to the unoccupied $d_{xy}$ component on a neighboring Ru site [a black solid arrow in Fig. 2(a)] and from the occupied $d_{yz/zx}$ to the unoccupied $d_{yz/zx}$ [a red solid arrow in Fig. 2(a)], respectively [17]. In $E\|c$, there is no clear peak structure below the charge-transfer peak. The broad bump below the charge-transfer peak can be understood as the nonvanishing matrix element of transitions $\alpha$ and $\beta$ along the $c$ axis in the distorted structure. To the first order approximation, the high $T$ (295 K) paramagnetic state can be described by the mixture of AF and FM solutions from the first-principles calculations. As clearly noticed in $\sigma(\omega)$ at 295 K (FM), peaks $\alpha$ and $\beta$ are strongly affected by orbital and spin ordering, and follows the *similar trend* of experimental data (see Fig. 4). With elongation of $RuO_6$ octahedra and an increase of the FM component in the spin configuration at high $T$, the peak $\alpha$ [a black solid arrow in Fig. 2(b)] is strongly enhanced and moved to the lower energy region due to the increased $d_{xy}$ hole population as well as to the decreased Jahn-Teller splitting, while the peak $\beta$ [a red dashed arrow in Fig. 2(b)] is strongly suppressed due to spin flip transition.

Figures 4(a) and 4(b) show the experimental $\sigma(\omega)$ results of $Ca_2RuO_4$ for $E\|ab$ and $E\|c$, respectively. For both polarizations, there are appreciable $T$-dependent changes of the spectral weight at least up to 4 eV. The optical sum rule is satisfied near 4.5 eV, as demonstrated in the insets of Fig. 4 by the near convergence of an effective number of electrons, $N_{\rm eff}(\omega) = (2m_0)/(\pi e^2 N)\int_0^\omega \sigma(\omega')\,d\omega'$ at 10 K (thick lines) and 370 K (thin lines). Here $m_0$ is the free electron mass

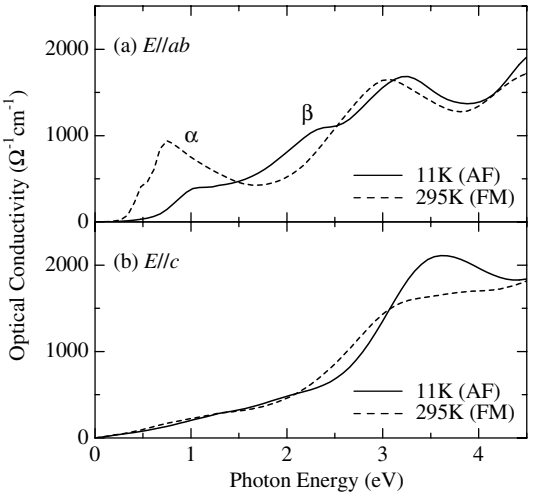


FIG. 3. Optical conductivity spectra $\sigma(\omega)$ obtained by LDA + $U$ calculation at 11 K (AF) (solid lines) and 295 K (FM) (dashed lines) for (a) $E\|ab$ and (b) $E\|c$. $\alpha$ and $\beta$ are the optical transitions as assigned in Fig. 2.

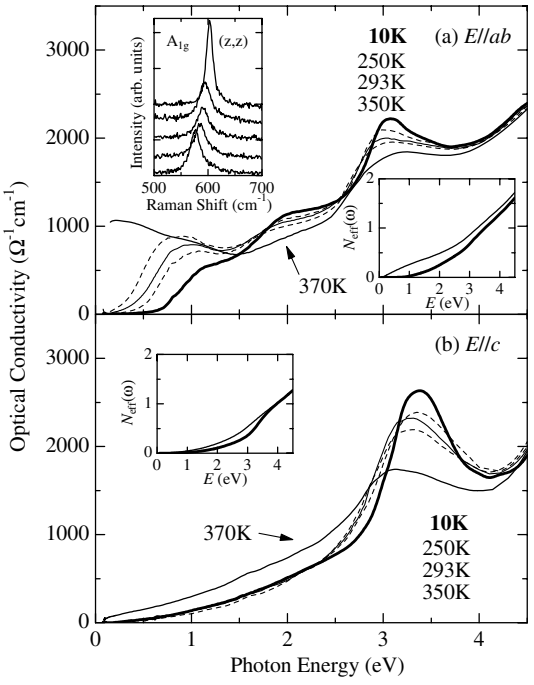


FIG. 4. Temperature $T$-dependent optical conductivity spectra $\sigma(\omega)$ for (a) $E\|ab$ and (b) $E\|c$. In the insets of (a) and (b), we show the effective number of electrons $N_{\rm eff}(\omega)$ at 10 K (thick lines) and 370 K (thin lines). The $T$-dependent (10, 250, 293, 350, and 370 K from top to bottom) Raman scattering spectra with $A_{1g}$ symmetry are also shown in the inset of (a). For clarity, the intensity levels are shifted for each $T$.

and $N$ the number of formula units (i.e., the number of Ru atoms). For $E\|ab$, a clear gap feature is observed below 1.5 eV for $T < T_{MI}$ ( $\equiv$ 363 K). With the increase of $T$, the spectral weight above 1.5 eV is transferred to a lower energy region and for $T > T_{MI}$ (e.g., $T = 370$ K) the gap structure is fulfilled, giving rise to a metallic feature [18]. For $E\|c$, the spectral weight above 3.0 eV is transferred to a lower energy region as well with the increase of $T$. However, a metallic response, i.e., a large spectral weight in the low energy region down to zero energy, is not observed. This feature is similar to that of $Sr_2RuO_4$ at the normal state [19], indicating a quasi-2D metallic state. For more quantitative analyses of the spectral weight transfer and the metal-insulator transition, we deduced the $T$ dependence of $N_{\rm eff}$ at 1.5 eV, where $\sigma$ values of 10 and 370 K are nearly the same (i.e., isosbetic point), and the optical gap $2\Delta$, which was defined as the crossing point on the abscissa with linear extrapolation of $\sigma(\omega)$. As shown in Fig. 1(c), there appears a close correlation between $N_{\rm eff}$ (1.5 eV) (solid circles) and $2\Delta$ (solid squares).

In accord with the large change of electronic structure, the Raman phonon mode corresponding to apical oxygen stretching vibration [20] also shows a large variation with $T$. In the inset of Fig. 4(a), we show the $T$-dependent Raman scattering spectra with $A_{1g}$ symmetry for $(z, z)$ configuration. There is an apical oxygen stretching mode near 600 $cm^{-1}$ at 10 K [21] without any splitting or another stretching mode as compared with that at 370 K ( $> T_{MI}$). Its frequency ($\omega_{\rm ph}$) shows an appreciable redshift with increasing $T$ [open circles in Fig. 1(b)]. The result suggests the increase of a Ru-O bond length along the $c$ axis with $T$ being consistent with that of the neutron scattering experiment [5].

Systematic variations of electronic structure and phonon frequency shown in Figs. 1(b) and 1(c), as well as our band calculation shown in Fig. 2, clearly indicate a key role of $d_{xy}$ orbital ordering stabilized by the Jahn-Teller distortion of $RuO_6$ octahedra and Coulomb repulsion. The $d_{xy}$ orbital ordering which is nearly saturated below $T_N$ results in the small effective number of electrons $N_{\rm eff}$ (1.5 eV), the large optical gap $2\Delta$, and the high apical phonon mode frequency $\omega_{\rm ph}$. Destabilization of the $d_{xy}$ orbital ordering with increasing $T$ causes the increase of $d_{xy}$ hole density (or decrease of $d_{yz/zx}$ hole density) and the elongation of $RuO_6$ octahedra. It results in the increase of $N_{\rm eff}$ (1.5 eV), decrease of $2\Delta$, and decrease of $\omega_{\rm ph}$ for $T_N < T < T_{MI}$. In accord with the structural transition, the increased bandwidth of the $d_{xy}$ orbital causes the $d_{xy}$ orbital disordering and, accordingly, the metal-insulator transition. It results in a sharp increase of $N_{\rm eff}$ (1.5 eV), a disappearance of $2\Delta$, and a sharp decrease of $\omega_{\rm ph}$ above $T_{MI}$. To reinforce our conclusion, we became aware that the superlattice peak, expected for antiferro-orbital ordering, was not observed in a recent resonant x-ray scattering experiment [22].

In summary, we have investigated the temperature-dependent optical conductivity spectra of $Ca_2RuO_4$. By combining the spectroscopic results with the transport and structural features as well as with the LDA + $U$ calculation, the crucial role of $d_{xy}$ orbital ordering is definitely shown for the large temperature variation of the electronic structure and the metal-insulator transition.

We thank N. Nagaosa and K. Terakura for helpful discussions, N. Takeshita for his help in the transport experiment, and M. Kubota and Y. Murakami for informing us of the result of resonant x-ray scattering prior to publication.

[1] S. Nakatsuji and Y. Maeno, Phys. Rev. Lett. **84**, 2666 (2000).
[2] Y. Maeno *et al.*, Nature (London) **372**, 532 (1994).
[3] S. Nakatsuji, S. Ikeda, and Y. Maeno, J. Phys. Soc. Jpn. **66**, 1868 (1997).
[4] G. Cao *et al.*, Phys. Rev. B **56**, R2916 (1997); C. S. Alexander *et al.*, *ibid.* **60**, R8422 (1999).
[5] O. Friedt *et al.*, Phys. Rev. B **63**, 174432 (2001).
[6] S. Nakatsuji and Y. Maeno, Phys. Rev. B **62**, 6458 (2000).
[7] V. I. Anisimov *et al.*, Eur. Phys. J. B **25**, 191 (2002).
[8] Z. Fang and K. Terakura, Phys. Rev. B **64**, 020509(R) (2001).
[9] T. Mizokawa *et al.*, Phys. Rev. Lett. **87**, 077202 (2001).
[10] T. Hotta and E. Dagotto, Phys. Rev. Lett. **88**, 017201 (2002).
[11] J. S. Lee *et al.*, Phys. Rev. Lett. **89**, 257402 (2002).
[12] The similar drops of $\chi_{ab}$ and $\rho_{ab}$ using flux-grown sample were also reported in Ref. [4]. However, the transition is not so clear perhaps due to the microcracks of their sample, as the authors clarified.
[13] G. Cao *et al.*, Phys. Rev. Lett. **78**, 1751 (1997).
[14] The value of $U_{\rm eff}$ merely represents the parameter to fit the experimental gap. See Z. Fang and K. Terakura, J. Phys. Condens. Matter **14**, 3001 (2002).
[15] M. Braden *et al.*, Phys. Rev. B **58**, 847 (1998).
[16] Z. Fang and N. Nagaosa (to be published).
[17] Lee *et al.* [Ref. [11]] explained the origin of two $d$-$d$ transition peaks in terms of the antiferro-orbital ordering. However, they did not consider the important modification of electronic structure by the rotation/tilting of $RuO_6$ octahedra and the resultant strong hybridization between the $d_{xy}$ and $d_{yz/zx}$ states on the neighboring sites.
[18] The intensity of $\sigma$ slowly decreases with $\omega$, which is reminiscent of a bad metallic behavior. See A. V. Puchkov *et al.*, Phys. Rev. Lett. **81**, 2747 (1998).
[19] T. Katsufuji, M. Kasai, and Y. Tokura, Phys. Rev. Lett. **76**, 126 (1996).
[20] S. Sakita *et al.*, Phys. Rev. B **63**, 134520 (2001).
[21] Existence of one stretching mode suggests the same Ru-O(2) bond length in a unit cell might be consistent with ferro-orbital ordering.
[22] M. Kubota *et al.* (unpublished); Bull. Jpn. Phys. Soc. **57**, 489 (2002).